Effect of Branched PP Content on the Physical Properties and Cell Growth During Foaming of TPOs

Tara J. McCallum,[1] Marianna Kontopoulou,[1] Chul B. Park,[2] Anson Wong,[2] Seong G. Kim[2]

[1]*Department of Chemical Engineering, Queen's University, Kingston ON K7L 3N6, Canada*
[2]*Department of Mechanical and Industrial Engineering, University of Toronto, Toronto ON M5S 3G8, Canada*

Received 4 January 2008; accepted 5 April 2008
DOI 10.1002/app.28648
Published online 10 July 2008 in Wiley InterScience (www.interscience.wiley.com).

ABSTRACT: Linear/branched PP blends at various ratios were used as the matrix for thermoplastic olefin (TPO) compounds, containing an ethylene–octene copolymer dispersed phase. A detailed investigation of the physical properties of these blends revealed that addition of branched PP (BPP) resulted in improved stiffness and flexural properties. Given that the phase morphology of the blends and the interfacial tension between their components remained virtually unaffected, these improvements are attributed to the higher stiffness of the BPP-containing matrices. Talc-filled TPOs containing branched PPs exhibited further improvements in the stiffness and flexural properties. An investigation into the bubble growth process during foaming using a batch foaming simulation system revealed that the presence of BPP resulted in a slight delay in cell nucleation, whereas the rate of bubble growth was not significantly altered.
 J Appl Polym Sci 110: 817–824, 2008

Key words: PP; branched; thermoplastic olefin; properties; foaming

INTRODUCTION

Thermoplastic Olefin (TPO) blends, produced by combining polypropylene (PP) with an elastomer, are capable of displaying a broad range of properties, from rigid to soft, depending on the PP to elastomer ratio. Generally, the addition of an elastomeric component to PP aims at improving its low temperature impact strength and ductility. This usually comes at the expense of the tensile modulus and flexural properties. Both ethylene–propylene rubber (EPR) and ethylene–propylene–diene terpolymers (EPDM) have been used as the elastomeric compounds in numerous studies.[1–3] During the last decade polyolefin elastomers (POEs), synthesized by metallocene or single-site catalysts, are increasingly being used as the rubber phase in TPO blends, because of their relatively low molecular weights and thus improved processability compared with EPR and EPDM.[4–6] This characteristic is particularly favorable for impact modifications of low molecular weight PP.[7]

Although TPOs are usually produced with linear PP (LPP) homopolymers or copolymers, recent developments have highlighted interest for TPOs based on branched PPs, or mixtures of linear and branched PPs. The addition of long-chain branches onto a PP backbone has been shown to increase the melt strength of the material, therefore improving its thermoformability[8] and foamability.[9] In extrusion foaming it has been demonstrated that the branched PPs are better able to retard cell coalescence and increase the expansion ratio during foaming.[9,10] Reductions in density, homogeneous cell size distribution, and lower amounts of coalesced cells have been reported in LPP/BPP blends,[11–14] although these improvements depend largely on the processing conditions[9,11,12] and the LPP/BPP ratio.[13] The exact mechanism through which the branched structure affects the quality of the final foams is still unclear; it is uncertain whether in addition to the well-known prevention of cell coalescence, the branched structure affects the initial stages of bubble growth.

We have reported recently the rheological and physical properties of a series of linear and branched PP blends.[15] These materials exhibited pronounced strain hardening, on addition of small amounts of BPP. Given the potential benefits in automotive applications involving thermoformed and foamed products, it is of interest to investigate the properties of TPOs containing these blends as matrices. This article reports the morphology and mechanical properties of TPOs and TPO/talc composites containing various amounts of branched PP (BPP) in their matrix. We further investigate the influence of BPP content on the cell growth process of TPOs during

Correspondence to: M. Kontopoulou (marianna.kontopoulou@chee.queensu.ca).

foaming, using a batch foaming simulation system, which is capable of recording the initial stages of foaming,[16,17] thus differentiating between the bubble growth and cell coalescence stages.

EXPERIMENTAL

Materials

The PPs used in this study are two PP homopolymers supplied by Basell: a linear PP (LPP) resin (Pro-fax PD702, MFR at 230°C/2.16 kg, 35 g/10 min) and a high melt strength branched PP (BPP) resin (Pro-fax PF611, MFR at 230°C/2.16 kg, 30 g/10 min). The density of both PPs is 902 kg/m^3. The molecular weight and branch content of the PPs were measured using a Viscotek model 350 high temperature GPC, equipped with a dual angle LS (78 and 908) viscometer and RI detectors and are $M_n = 36.7$ kg/mol, $M_w/M_n = 8.4$ for the LPP; $M_n = 77.5$ kg/mol, $M_w/M_n = 6.6$, estimated average number of branches per molecule = 4.2 for the BPP.

The polyolefin elastomer was an ethylene–octene copolymer, Engage 8407, was supplied by The Dow Chemical Company. This material has an MFI (190°C/2.16 kg, g/10 min) of 30 and a density of 870 km/m^3. As outlined in the following section, a series of PP/POE samples (70/30 by weight) were prepared, with the PP matrix consisting of a range of BPP compositions (LPP/BPP 20/80, 40/60, 60/40, and 80/20 by weight).

Blend preparation

Blend components were dry blended with 0.2% antioxidant (Irganox B225 from CibaGeigy). Two compounding methods were utilized. Small amounts of samples, suitable for morphological characterization and foaming experiments were prepared using a DSM Xplore 5 mL twin-screw microcompounder, equipped with a conical corotating intermeshing twin-screw element.

Larger amounts, for use in mechanical testing, were prepared using a Haake Polylab Rheocord torque rheometer equipped with a Rheomix 610p mixing chamber and roller rotors until the torque profile reached steady state (approximately 6–7 min). The Haake was operated at approximately 70% capacity and 100 rpm. In both cases compounding took place under a nitrogen blanket to limit PP degradation. Compounding took place at 210°C for approximately 5 min.

Rheological characterization

The viscosity of the pure components and the blends was measured at a shear rate range of (20–2000 s^{-1}), using a Rosand RH2000 twin bore capillary rheometer (Malvern Instruments) at 210°C. The shear viscosities were calculated by applying the Bagley and Rabinowitch corrections.

The viscoelastic properties were characterized in the shear oscillatory mode, using a controlled stress rheometer (ViscoTech by Rheologica) equipped with parallel plates 20 mm in diameter. The measurements were performed at a gap of 0.5 mm and a temperature of 180°C, under nitrogen blanket. Samples used in the rheometer were compression molded discs, approximately 2 mm in thickness and 25 mm in diameter and were prepared using a Carver hydraulic press, heated at 200°C.

Scanning electron microscopy

A JEOL JSM-840 scanning electron microscope was used to characterize the morphology of the blends. Compression molded samples were freeze-fractured under liquid nitrogen and etched in toluene for 2 h. The fracture surfaces were sputtered with gold before viewing under the microscope. Image analysis was performed using the Sigma-Scan Pro software.

Mechanical properties

Compression molded sheets were prepared using a Carver hydraulic press, heated to 200°C, and type V specimens were then stamped out of the sheets, according to the ASTM D638 standard. An Instron Universal Tester, model 3369, was used to determine the tensile properties of all the materials. Five replicate runs at a crosshead speed of 50 mm/min were completed at each composition to ensure the reproducibility of the results.

Flexural tests were also performed using the Instron 3369, in accordance with ISO 178, at a strain rate of 5 mm/mm/min. The samples having dimensions 80 × 10 × 4 mm^3 were compression molded at 200°C with the hydraulic press. The flexural modulus as well as flexural stresses and strains were calculated from the resulting curves.

The impact strength of the blends was tested using an Instron Izod impact testing apparatus, equipped with a 3.95 kg hammer at room temperature and at −20°C. Specimens were injection molded with dimensions of 64 × 12.7 × 5 mm^3 and notched. Measurements were performed according to ASTM D256. Samples tested at low temperatures were conditioned in a freezer overnight. Tests were repeated three times for each experimental condition.

Foaming visualization and analysis

Foaming visualization experiments were conducted using a batch foaming simulation system, which has

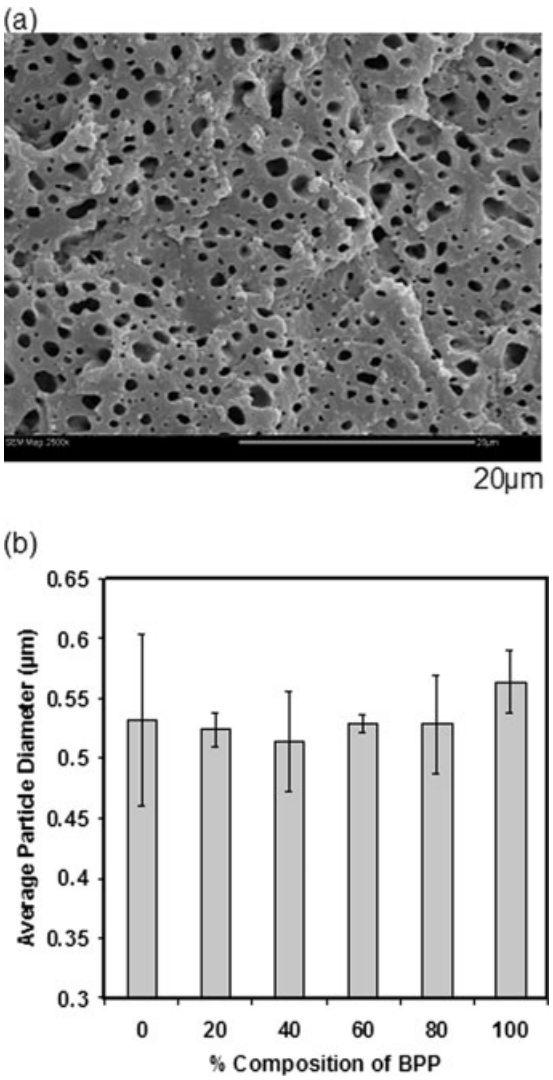

Figure 1 (a) Representative SEM image of TPOs prepared in the microcompounder (magnification ×2500); (b) Average particle diameter for TPOs prepared in the microcompounder, as a function of BPP content.

been described in detail previously.[16,17] The temperature and pressure in the simulation chamber were regulated using a thermostat and a syringe pump, respectively. An ADAC board was used to record the pressure drop during experimentation, whereas a high speed CCD camera was used to record the foaming process.

The foaming experiments were performed on blends prepared in the microcompounder. Disks having dimensions 7 mm in diameter and 200 μm in thickness were prepared by compression molding using a Carver hydraulic press, heated at 200°C. The disks were then placed into the simulation chamber, which chamber was set to 180°C, under a pressure of 2000 psi, using nitrogen as the blowing agent. The maximum pressure drop rate for all experiments was 33 MPa/s. A program based on Labview was used to open the solenoid valve and record the pressure decay, while simultaneously, the CCD camera recorded the bubble behavior. For each condition, three separate experiments were run, and the images were analyzed using the Sigma Scan Pro 5.0 image analysis software. Averages of these runs are reported.

RESULTS

Blend morphology

We first begin by an examination of the morphological characteristics of the blends, as it is well known that morphology influences the mechanical properties and possibly the foaming behavior. These blends are immiscible and in accordance with previous findings[4–7] they have a droplet matrix morphology, as depicted by the representative SEM image shown in Figure 1(a). The blends prepared in the microcompounder have very similar average particle size of around 0.5 μm, irrespective of the PP matrix composition [Fig. 1(b)]. It should be noted that the blends compounded in the batch mixer were coarser, with an average particle size of 1.5 μm, highlighting the importance of the mixing environment when compounding these materials.

Examination of the shear viscosities of the materials shown in Figure 2 revealed that, although the BPP has substantially higher molecular weight than LPP (77.5 kg/mol and 36.7 kg/mol, respectively), the shear viscosities of both materials at high shear rates are very comparable. This is because of the higher degree of shear thinning of the BPP material. Consequently, the viscosity ratio between the PP matrix and the dispersed phase is the same for all LPP/BPP ratios, resulting in similar particle breakup characteristics. The addition of BPP affects the elasticity of the matrix as well, as reported earlier,[15] but this apparently did not affect particle breakup,

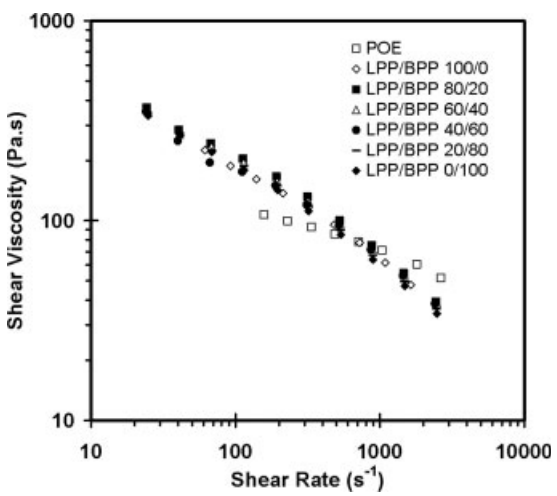

Figure 2 Shear viscosity as a function of shear rate for the PP blends and the POE at 210°C.

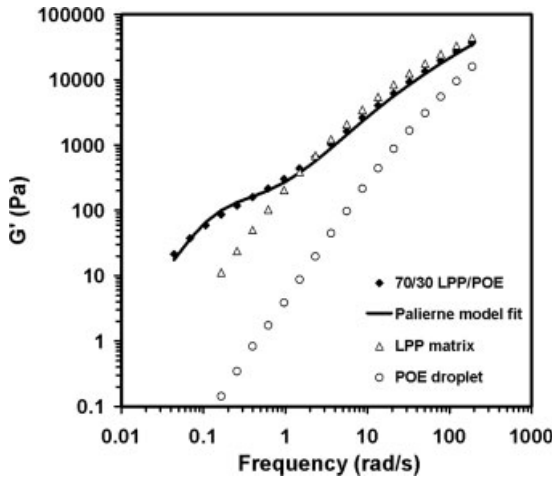

Figure 3 Representative fit of the Palierne model for 70/30 wt % LPP/POE blends.

at least at the shear rates relevant to compounding in this work.

Given the importance of interfacial tension on the morphology and the properties of immiscible polymer blends, it is also of interest to investigate whether addition of BPP alters the interfacial tension between the PP matrix and the elastomer dispersed phase. It should be noted that our previous work on linear/branched PP blends[15] has revealed that LPP and BPP are miscible in the melt state; therefore the molten PP matrix should behave as a single phase system. The interfacial tension was estimated by fitting the Palierne emulsion model[18,19] to the viscoelastic data obtained through oscillatory shear measurements, for the simplified case where the polydispersity of the dispersed droplets is less than 2.[9] A representative illustration of the Palierne model fit for a TPO containing 30 wt % POE as the dispersed phase, with the matrix containing 100% LPP is shown in Figure 3. Based on the Palierne model estimates the interfacial tension values do not vary significantly; the TPOs containing 100% LPP in their matrix have an interfacial tension of 0.103 mN/m, whereas those containing 100% branched PP arrive at a value of 0.072 mN/m. All other compositions fell in-between. It should be noted that these values are very low, in agreement with previous findings on similar PP/POE systems,[7] suggesting excellent compatibility between the two phases.

Mechanical properties

As expected, the addition of 30 wt % of POE in the PP matrix decreased substantially the tensile (Young's) modulus of the material [Fig. 4(a)]. At the same time, the elongation at break increased, as the PP matrix displayed elongations below 30%, whereas all the TPOs had elongations at break above 100% [Fig. 4(b)].

What is more noteworthy is that the trends reported for linear/branched PP blends in our earlier work[15]; whereby small additions of BPP generated a stiffer material, persist in the TPOs, as shown in Figure 4(a). This is also reflected from the flexural properties in Figure 5, which demonstrate that all materials containing BPP have a higher flexural modulus. Given that there are no notable differences in the morphology and the interfacial tension of the blends, this behavior is attributed to the matrix properties. As demonstrated by McCallum et al.[15] the BPP used in this work is stiffer and more brittle compared with the LPP. Its heat of fusion is also slightly higher, translating into a higher crystallinity, contrary to what would be expected for a branched material, possibly because of its higher molecular weight. The same trend persists in the TPOs, as shown in Table I. This finding reveals the benefits of using BPP, which enables the use of a higher

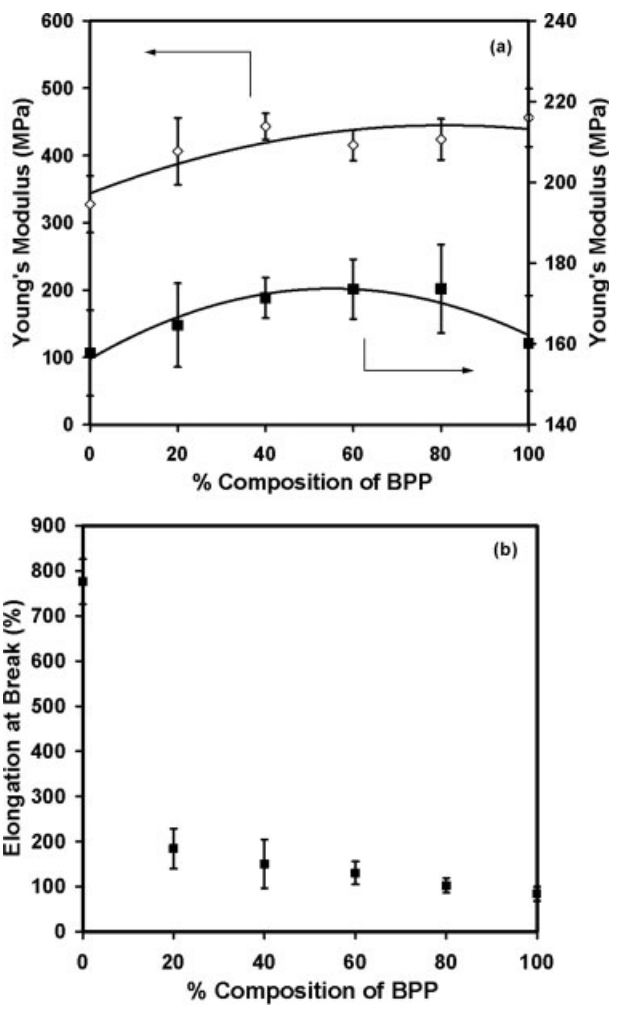

Figure 4 (a) Young's moduli and (b) elongation at break as a function of BPP content; ◇, PP blends; ■, TPOs. Lines are drawn to guide the eye.

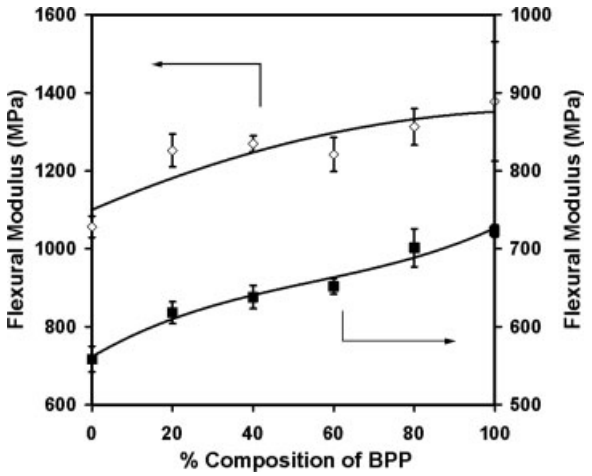

Figure 5 Flexural modulus as a function of BPP content; ◇, PP blends; ■ TPOs. Lines are drawn to guide the eye.

molecular weight material, thus offering improved mechanical properties, without sacrificing its processability (see also Fig. 2).

As shown in Figure 4(b) the beneficial effect of BPP addition on the stiffness comes at the expense of the elongation at break. Nevertheless, out of all the blends prepared in this study, none failed during notched Izod impact tests conducted at ambient temperature, whereas at −20°C, the TPO sample containing 100% branched PP as the matrix failed with an impact energy of 0.011 J/m^2. This implies that the toughness does change on addition of BPP, but overall the reduction in impact energy does not result in sample failures during Izod impact testing.

Effect of talc

The tensile properties and flexural properties of blends prepared with varying levels of branched PP, as well as talc, are represented in Figures 6 and 7, respectively. The addition of talc clearly increases the Young's and flexural moduli of the material by as much as twofold, at a 20% talc loading. The substantial gains in all flexural properties when talc is added in the TPOs, are shown in Figure 7. The tensile properties of the composites were not affected significantly by the amount of branched PP used,

TABLE I
Heats of Fusion of TPOs Containing Varying Levels of BPP

BPP matrix content (wt. %)	Heat of fusion (J/g)
0%	64.01
20%	71.07
40%	69.60
60%	72.06
80%	70.82
100%	71.51

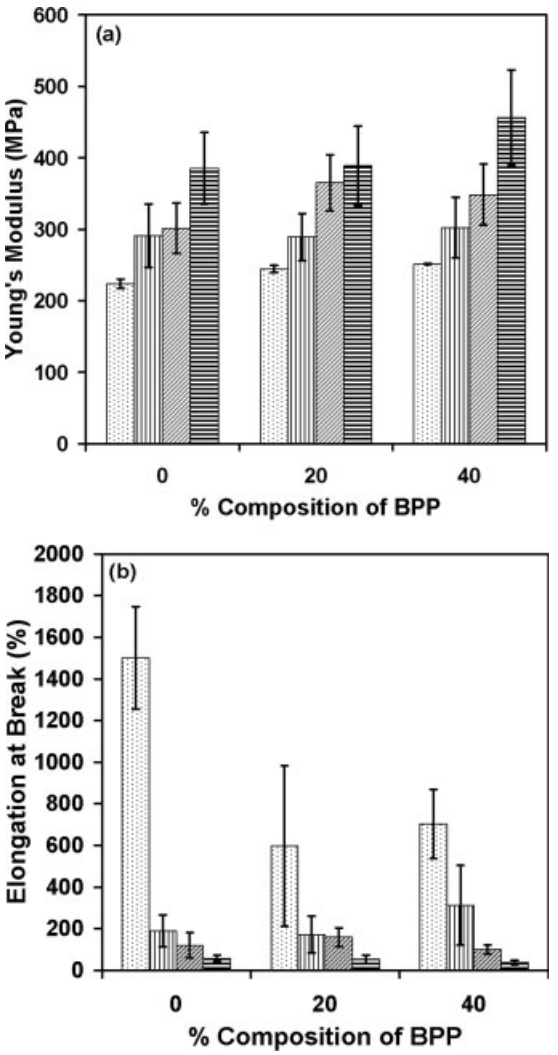

Figure 6 (a) Young's moduli and (b) elongation at break as a function of BPP content; ⋮⋮, 0 wt % talc; ||||, 5 wt % talc, ▨, 10 wt % talc; ▤, 20 wt % talc.

whereas the flexural properties generally benefited from the presence of BPP, up to a 60% BPP content, where a notable decrease in flexural strain occurred (Fig. 8). The notched izod impact tests performed show failures at −20°C of the composites containing 5 wt % talc with 0 or 20 wt % BPP, with impact energies of 0.0108 and 0.0132 J/m^2, respectively. None of the samples failed at room temperature.

Foaming visualization and analysis

Representative images captured during batch foaming of TPOs containing 30 wt % POE can be seen in Figure 9. Image analysis was used to determine the cell densities with respect to the unfoamed volume (N_{unfoamed}), according to eqs. (1–3):[16]

$$N_{\text{unfoamed}}(t) = \left(\frac{N(t)}{A_c}\right)^{3/2} \times \text{VER}(t) \quad (1)$$

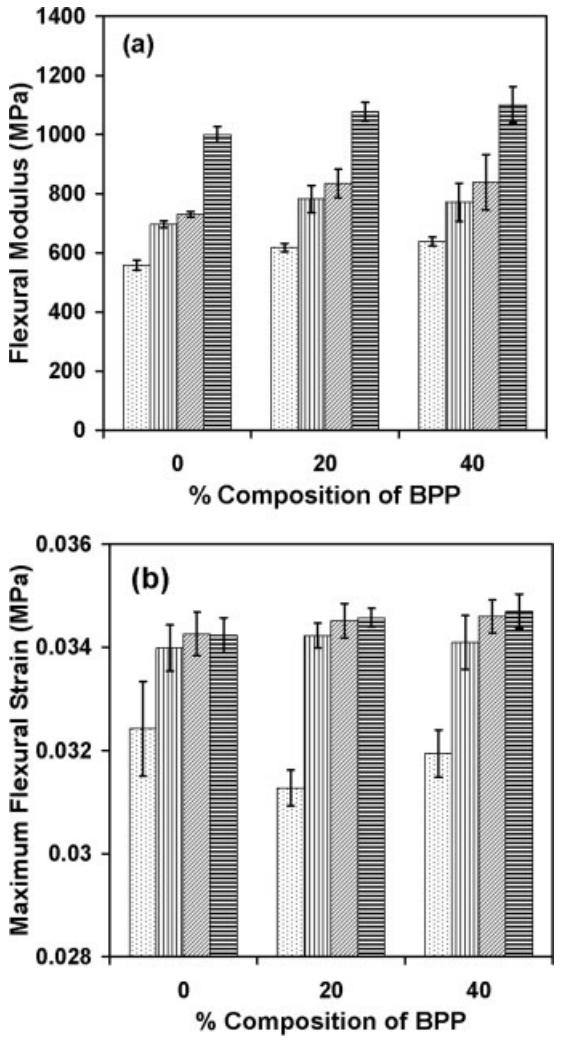

Figure 7 (a) Flexural moduli and (b) flexural strains as a function of BPP content; ⋮⋮, 0 wt % talc; ||||, 5 wt % talc; ▨, 10 wt % talc; ▤, 20 wt % talc.

The volume expansion ratio (VER) is:

$$\mathrm{VER}(t) = 1 + \left(\frac{4}{3}\pi\left(R_{\mathrm{avg}}(t)\right)^3 \times N(t)\right) \qquad (2)$$

where $N(t)$ is the number of bubbles observed, A_c is the analysis area, and R_{avg} is the average radius of the observed bubbles.

In the case of the batch foaming experiments, the observations are made only for the initial growth stage, and therefore the VER is approximately equal to 1. Hence, the expression for N_{unfoamed} can be reduced to:

$$N_{\mathrm{unfoamed}}(t) = \left(\frac{N(t)}{A_c}\right)^{3/2} \qquad (3)$$

Cell density versus time curves for TPOs containing LPP/BPP matrices are shown in Figure 10. The two observations that must be noted are that in the presence of BPP cell nucleation is generally delayed, but once it does occur, the rate of cell growth is similar for all compositions. Similar results were obtained during foaming of the talc-filled TPOs.

Foaming of immiscible blends, such as the TPOs used in this work, involve complex phenomena. In addition to the cell nucleation, growth and stabilization/cell coalescence mechanisms, foaming of blends is also influenced by the individual components' rheological[20] and thermal properties,[21] the blend morphology,[20–23] as well as the diffusivity/solubility of the gases in the respective blend components.[17,20,24] Interfacial tension between the immiscible blend phases may also play a role. The TPOs used in this work have very similar morphologies and interfacial tension, as well as the same type of dispersed phase; therefore, the only factors that should affect cell growth are the rheological properties of the matrix and the gas solubility in the melts.

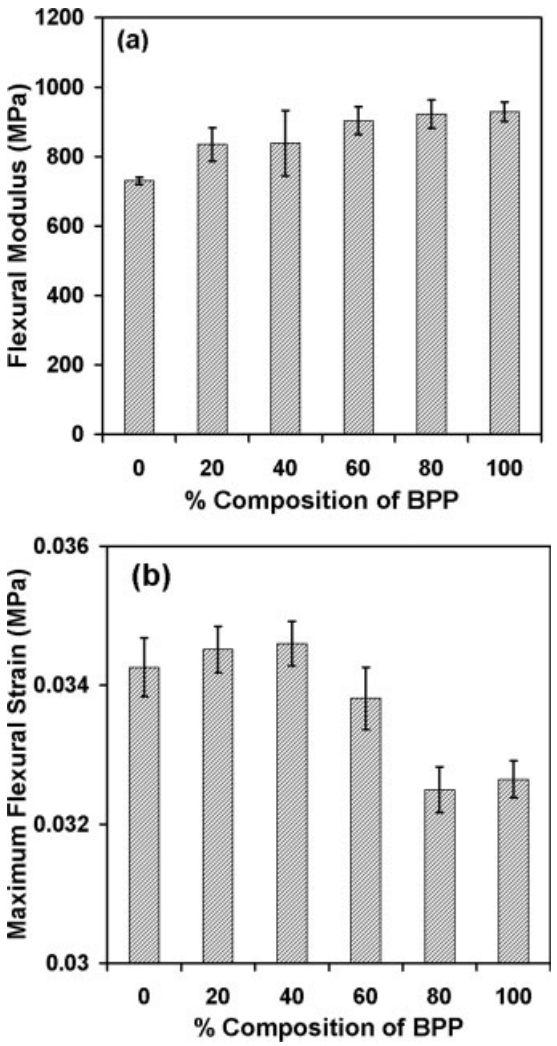

Figure 8 (a) Flexural moduli and (b) flexural strains for the POE blends containing 10 wt % talc as a function of BPP content.

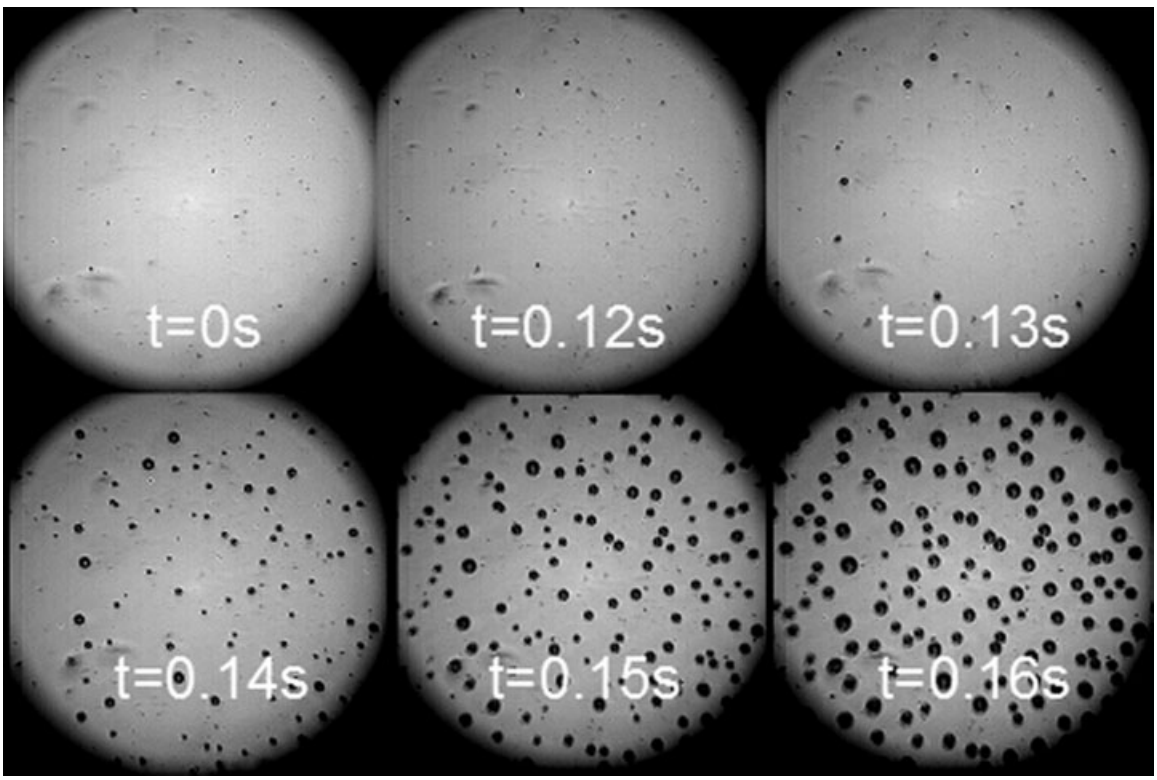

Figure 9 Representative images captured during the batch foaming experiments of TPOs containing 100 wt % LPP using nitrogen as a blowing agent; $P_{sat} = 2000$ psi, 180°C, $dP/dt = 33$ MPa/s.

Both the rheology and gas solubility are known to be influenced by the presence of a branched component. Li et al.[25] demonstrated that the solubilities of CO_2 and N_2 physical blowing agents are lower in BPP, because of its entangled molecular chain structure. This results in LPP generally nucleating more cells than BPP when the same pressure is used[13] and can explain the trends shown in Figure 10.

Once nuclei form, the rate of cell growth is not substantially different between the various blend compositions. As shown previously,[15] the PP blends used as matrices for the TPOs under consideration in this work showed significantly increased strain hardening, as well as higher low-frequency melt elasticity, at the addition of BPP amounts as low as 20 wt %. However, the strain hardening of the blends containing BPP obviously did not influence significantly the rate of individual cell growth, as shown in Figure 10. This is in agreement with the findings by Otsuki and Kanai,[26] who indicated that the most relevant rheological parameter for the growth rate process is the high-frequency elastic modulus data. Indeed, the high frequency elastic moduli for our PP blends are very similar.[15] Therefore, the cell growth stage is not influenced by the strain hardening of the matrix, and the only important factor governing the process is the rate of nuclei growth, which depends on the solubility of the blowing agent in the melt.

Based on the results of this work, and given that we have been able to separate and monitor only the cell growth mechanism, we can state that the previously reported improvements in foam quality in the presence of BPP[10] are only because of the prevention of cell coalescence during the final stages of foaming in agreement with the model predictions of Taki et al.[27] and are not attributed in any way to enhancements in the bubble growth rate.

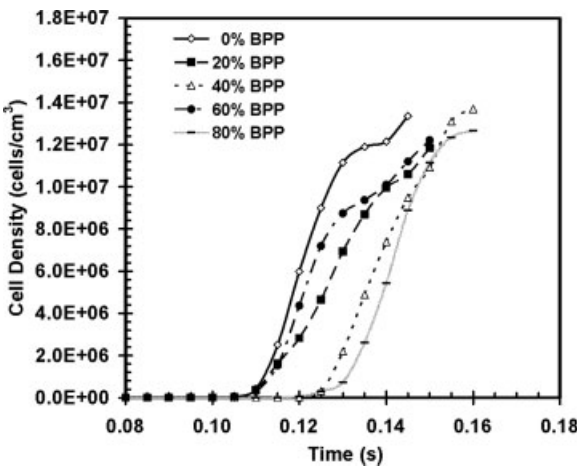

Figure 10 Cell density as a function of time for TPOs containing various amounts of BPP in their matrix.

CONCLUSIONS

Addition of branched PP in TPOs did not alter significantly the morphology or the interfacial tension between the blend components. All materials containing branched PP were generally more rigid and had enhanced flexural properties. However, these qualities came at the expense of the elongation at break. All blends showed excellent low temperature toughness. The addition of talc to TPO blends causes further gains in the stiffness and flexural properties of the blends.

Investigation of the initial bubble growth stage during batch foaming experiments revealed that the rate of cell growth was not affected by the presence of the branched polyolefin. However, the nucleation rate was slower in the presence of the branched component, apparently due to the lower solubility of the gas in the presence of branching in the melt.

References

1. D'Orazio, L.; Cecchin, G. Polymer 2001, 42, 2675.
2. Karger-Kocsis, J.; Kalló, A.; Kuleznev, V. N. Polymer 1984, 25, 279.
3. van der Wal, A.; Mulder, J. J.; Oderkerk, J.; Gaymans, R. J. Polymer 1998, 39, 6781.
4. Da Silva, A. L. N.; Tavares, M. I. B.; Politano, D. P.; Coutinho, F. M. B.; Rocha, M. C. G. J Appl Polym Sci 1997, 66, 2005.
5. Kukaleva, N.; Jollands, M.; Cser, F.; Kosior, E. J Appl Polym Sci 2000, 76, 1011.
6. McNally, T.; McShane, P.; Nally G. M.; Murphy, W. R.; Cook, M.; Miller, A. Polymer 2002, 43, 3785.
7. Kontopoulou, M.; Wang, W.; Gopakumar, T. G.; Cheung, C. Polymer 2003, 44, 7504.
8. Gotsis, A. D.; Zeevenhoven, B. L. F.; Hogt, A. H. Polym Eng Sci 2004, 44, 973.
9. Naguib, H. E.; Park, C. B.; Hesse, A.; Panzer, U. Polym Eng Sci 2002, 42, 1481.
10. Park, C. B.; Cheung L. K. Polym Eng Sci. 1997, 37, 1.
11. Nam, G. J.; Yoo, J. H.; Lee, J. W. J App Polym Sci 2003, 96, 1793.
12. Reichelt, N.; Stadlbauer, M.; Folland, R.; Park, C. B.; Wang, J. Cell Polym 2003, 22 315.
13. Spitael, P.; Macosko, C. W. Polym Eng Sci 2004, 44, 2090.
14. Stange, J.; Munstedt, H. J Cell Plast 2006, 42, 445.
15. McCallum, T. J.; Kontopoulou, M.; Park, C. B.; Muliawan, E. B.; Hatzikiriakos, S. G. Polym Eng Sci 2007, 47, 1133.
16. Guo, Q.; Wang, J.; Park, C. B.; Ohshima, M. Ind Eng Chem Res 2006, 45, 6153.
17. Leung, S. N.; Park, C. B.; Xu, D.; Li, H.; Fenton, R. G. Ind Eng Chem Res 2006, 45, 7823.
18. Palierne, J. F. Rheol Acta 1990, 29, 204.
19. Graebling, D.; Muller, R.; Palierne, J. F. Macromol 1993, 26, 320.
20. Taki, K.; Nitta, K.; Kihara, S.-I.; Ohshima, M. J App Polym Sci 2005, 97, 189.
21. Lee, P. C.; Wang, J.; Park, C. B. Ind Eng Chem Res 2006, 45, 175.
22. Tejeda, E. H.; Sahagun, C. Z.; Gonzalez-Nunez, R.; Rodrigue, D. J Cell Plast 2005, 41, 417.
23. Kim, S. G.; Park, C. B.; Sain, M. SAE 2007 World Congress 2007, paper #07M-8, Detroit, MI.
24. Doroudiani, S.; Park, C. B.; Kortschot, M. T. Polym Eng Sci 1998, 38, 1205.
25. Li, G.; Wang, J.; Park, C. B.; Simha, R. J Polym Sci Part B: Polym Phys 2006, 45, 2497.
26. Otsuki, Y.; Kanai T. Polym Eng Sci 2005, 45, 1277.
27. Taki, K.; Tabata, K.; Kihara S.; Ohshima, M. Polym Eng Sci 2006, 46, 680.